



## LJMU Research Online

Turner, ML, Falkingham, PL and Gatesy, SM

**What is Stance Phase On Deformable Substrates?**

<http://researchonline.ljmu.ac.uk/id/eprint/16593/>

### Article

**Citation** (please note it is advisable to refer to the publisher's version if you intend to cite from this work)

**Turner, ML, Falkingham, PL and Gatesy, SM (2022) What is Stance Phase On Deformable Substrates? Integrative and Comparative Biology. ISSN 1540-7063**

LJMU has developed **LJMU Research Online** for users to access the research output of the University more effectively. Copyright © and Moral Rights for the papers on this site are retained by the individual authors and/or other copyright owners. Users may download and/or print one copy of any article(s) in LJMU Research Online to facilitate their private study or for non-commercial research. You may not engage in further distribution of the material or use it for any profit-making activities or any commercial gain.

The version presented here may differ from the published version or from the version of the record. Please see the repository URL above for details on accessing the published version and note that access may require a subscription.

For more information please contact [researchonline@ljmu.ac.uk](mailto:researchonline@ljmu.ac.uk)

<http://researchonline.ljmu.ac.uk/>

## **What is stance phase on deformable substrates?**

Morgan L. Turner<sup>1,2</sup>, Peter L. Falkingham<sup>3</sup>, Stephen M. Gatesy<sup>2</sup>

This is the submitted version of the manuscript, required by UK academic regulations to be uploaded to an institutional repository.

Please access the fully published, formatted manuscript at this link:

<https://academic.oup.com/icb/advance-article/doi/10.1093/icb/icac009/6552959>

## **What is stance phase on deformable substrates?**

Morgan L. Turner<sup>1,2</sup>, Peter L. Falkingham<sup>3</sup>, Stephen M. Gatesy<sup>2</sup>

<sup>1</sup>Department of Ecology, Evolution, and Organismal Biology, Division of Biology and Medicine, Brown University, Providence, RI, 02912, USA.

<sup>2</sup>Department of Computer Science and Engineering, University of Minnesota, Minneapolis, MN 55455, USA

<sup>3</sup>School of Biological and Environmental Sciences, Liverpool John Moores University, Liverpool, UK.

Author for correspondence: M. L. Turner; email: [turnerm@umn.edu](mailto:turnerm@umn.edu)

Running head: stance phase on deformable substrates

Keywords: kinematics, guineafowl, foot, XROMM, walking, biped

Total number of words in text: 5417

## Abstract

The stance phase of walking is when forces are applied to the environment to support, propel, and maneuver the body. Unlike solid surfaces, deformable substrates yield under load, allowing the foot to sink to varying degrees. For bipedal birds and their dinosaurian ancestors, a shared response to walking on these substrates has been identified in the looping path the digits follow underground. Because a volume of substrate preserves a 3-D record of stance phase in the form of footprints or tracks, understanding how the bipedal stride cycle relates to this looping motion is critical for building a track-based framework for the study of walking in extinct taxa.

Here we used biplanar X-ray imaging to record and analyze 161 stance phases from 81 trials of three Helmeted Guineafowl (*Numida meleagris*) walking on radiolucent substrates of different consistency (solid, dry granular, firm to semi-liquid muds). Across all substrates, the feet sank to a range of depths up to 78% of hip height. With increasing substrate hydration, the majority of foot motion shifted from above to below ground. Walking kinematics sampled across all stride cycles revealed six sequential gait-based events originating from both feet, conserved throughout the spectrum of substrate consistencies during normal alternating walking. On all substrates that yielded, five sub-phases of gait were drawn out in space and formed a loop of varying shape. Given the gradational nature and two-footed origins of such complex subsurface foot motion during normal alternating walking and some atypical walking behaviors, we discuss the definition of “stance phase” on deformable substrates. We also discuss implications of the gait-based origins of subsurface looping on the interpretation of locomotory information preserved in fossil dinosaur tracks.

## Introduction

Traditionally, a walking limb's movement during each stride cycle is temporally divided into stance and swing phases. On solid surfaces, the division is relatively unambiguous: stance phase occurs during foot-ground contact (also referred to as the “weight bearing” phase), and swing phase occurs while the foot is raised. For walking humans, stance phase has been further subdivided by a series of two-leg contact events defining double and single legged support (Gage et al., 1995). These few defining kinematic events create a framework through which the complexities of human (Murray, 1967; Winter, 1980; Whittle, 1996; Kuo et al., 2005) and avian (Verstappen et al., 2000; Daley and Birn-Jeffery, 2018) bipedal gait biomechanics have been modeled.

On deformable substrates, however, the ground yields with each step. If the substrate deforms plastically (i.e. the deformation is not elastically recovered), a footprint, or track, is made (Allen, 1989; Falkingham et al., 2011; Falkingham, 2014). Previous studies have revealed that with increasing substrate deformability, greater subsurface foot motions occur, and increasingly larger volumes of substrate are impacted (Milàn, 2006; Hatala et al., 2018; Gatesy and Falkingham, 2020; Falkingham et al., 2020). These volumes of substrate can preserve a record of complex foot movements through space and time. Thus, recognizing features in these

fossil tracks and understanding how they relate to patterns of bipedal locomotion is critical for building a track-based framework for the study of walking in extinct taxa.

In the case of the non-avian theropods, skeletal and track fossil material has documented the conservation of foot anatomy and bipedal parasagittal hind limb throughout the 240-million-year line to birds (e.g., Hutchinson, 2006). This makes Theropoda an ideal clade to study through the lens of experimental studies. In this clade, not only have general kinematic similarities to modern birds been documented from fossil tracks (Padian and Olsen, 1989; Gatesy et al 1999), but a shared looping pattern, more complex than merely stamping into the mud, has been identified (Turner et al., 2020; Falkingham et al., 2020). This shared looping response has formed the foundation for a framework for interpreting features in fossilized penetrative tridactyl tracks (Gatesy and Falkingham, 2020; Turner et al., 2020; Falkingham et al., 2020). The foot's overall sub-surface motion is generated by a combination of forward sinking and backward withdrawal. However, how loop geometry is formed in relation to the interplay between two feet during bipedal walking remains unclear.

Here, we apply biplanar X-ray videography to visualize and measure the sub-surface pedal kinematics of Helmeted Guineafowl. As kinematic patterns are ideally investigated by sampling broad locomotor diversity (Turner and Gatesy, 2021), a primary goal of this study was to generate as much variation in subsurface foot motion during walking as possible by presenting birds with a spectrum of substrate consistencies (solid, dry granular, and cohesive muds ranging in hydration, homogeneity, and compactness). As such, all analyzable trials in which guinea fowl exhibited walking were included in this study. We describe patterns in the path taken by the tip of the third digit—the dominant and central toe of functionally tridactyl feet—above and below ground. Due to the substantial variation in subsurface foot motion, we established homologous kinematic events of bipedal gait to compare walking steps across the continuum of substrates. Given the gradational nature and two-footed origins of such complex subsurface foot motion during normal alternating walking and some atypical walking behaviors, we discuss the definition of “stance phase” on deformable substrates. We also discuss implications of the gait-based origins of subsurface looping on the interpretation of locomotory information preserved in fossil dinosaur tracks.

## **Material and Methods**

The methods of data acquisition follow those described in Turner et al., (2020), and are summarized below.

### **Animals, substrates, and recording**

Biplanar X-ray data were collected from three adult Helmeted Guineafowl (*Numida meleagris*) obtained from a local breeder and housed at Brown University's Animal Care Facility. All animal experiments were conducted in accordance with the Institutional Animal Care and Use Committee of Brown University.

To allow for X-ray imaging of the pedal elements and markers below the ground surface (Fig. 1), substrates were chosen specifically for their radiolucency. Dry and wet substrates were contained in a plastic trough (20 cm deep x 30 cm wide x 125 cm long) filled to a depth of

approximately 18 cm to form a trackway, which was enclosed by a clear acrylic tunnel. A dry granular substrate was composed of ~1mm diameter poppy seeds (*Papaver somniferum*), used because they qualitatively behave like dry sand, while being more radiolucent (Li et al., 2013; Falkingham and Gatesy, 2014). Artificial mud was mixed from 60  $\mu$ m glass bubbles (K15, 3M Company, Maplewood, MN), Tennessee ball clay, and water, in a volume ratio of ~24:5:9. Mud consistency was adjusted by adding water, but evaporation, settling, and intentional layering precluded homogeneous properties within and between trials. Mud consistency ranged from very firm with low saturation to very mobile semi-liquid throughout the entire trough. Birds also walked across a solid trackway composed of a carbon fiber composite panel (foam core; 79 x 30.5 x 2.7 cm) placed on top of the trough, for comparative data.

Walking guineafowl were recorded at 250 fps by two X-ray cameras and two visible-light cameras in the W. M. Keck Foundation XROMM Facility at Brown University. Images for camera calibration and X-ray undistortion were collected with the same cameras. One bird had 2 mm disc-shaped lead markers fixed with cyanoacrylate adhesive beneath each claw and on the external surface of the tarsometatarsus (Fig. 1B).

### Point tracking and animation

Three-dimensional toe coordinates for the marked individual were extracted in XMALab (Gatesy et al., 2010; Knörlein et al., 2016) and animated in Maya 2020 (Autodesk Inc., San Rafael, CA, USA). For the unmarked birds, point rotoscoping (Ellis and Gatesy, 2013) was done in Maya using virtual camera calibrations and undistorted video from XMALab. Briefly, the reconstructed camera positions and undistorted X-ray video exported from XMALab were brought into Maya, where we created virtual cameras representing the real-world X-ray beams in three-dimensional space. A digital marker model was registered to the digit III ungual X-ray shadows of both videos by rotoscoping (Gatesy et al., 2010), and a csv file containing left and right digit III ungual (uDIII) coordinates for each frame was exported.

CT-based bone models were animated for several trials using a combination of marker-based X-ray reconstruction of moving morphology (Brainerd et al., 2010) and scientific rotoscoping (Gatesy et al., 2010).

### Kinematic events and motion pathlines

Individual stance phases within a trial were identified, sequentially numbered, and assigned a series of homologous kinematic events. Stance phases were determined by the first (**on**) and last (**off**) frames of uDIII substrate contact, based on observation of synchronized light video. While the tip of digit III (uDIII) was often the first point of ground contact, other digits occasionally made touchdown milliseconds earlier. Between **on** and **off**, the frame of each stance phase's maximum depth (**maxD**) separated sub-surface movements into **entry** (**on** to **maxD**) and **exit** (**maxD** to **off**). uDIII coordinates of both feet were extracted at event frames for the focal stance phase (**on**, **maxD**, **off**) as well as that of the opposite foot for both previous (**oppMaxD**, **oppOff**) and following steps (**oppOn**). These sets of coordinates were used to quantify the geometry of the loop created by this motion. All full and partial (containing only **on** or **off**, not both) stance phases were sampled.

Motion of uDIII was visualized as pathlines connecting claw positions at each frame. All uDIII pathlines are figured as left/right pairs in right-lateral view, progressing across the page

from left to right. Graphical representations of these paired foot data are color coded such that the focal stance foot is always red and the opposite foot is blue. Graphs were created in R (R Core Team, 2020). Rendered images and videos were produced in Maya 2020. All foot pose silhouettes are based on skeletal reconstructions or X-ray imaging of live animals. Figures were compiled in Adobe Illustrator version 24.3.

### **Measurements**

The substrate's surface was determined by the vertical position of uDIII at **on**, from which swing height (positive) and maximum depth (negative) are calculated. On deformable substrates, **entry** and **exit** motions create a subsurface loop between **on** and **off**. We calculate loop width as the horizontal distance between the most anterior extent of the uDIII **entry** path and most posterior extent of the uDIII **exit** path below the point of intersection.

### **Fossil specimens**

Fossil specimens included in this study were originally collected from the Lower Jurassic Portland Formation, Wethersfield (Wethersfield Cove), CT, USA and are housed in the Beneski Museum of Natural History at Amherst College, Amherst, MA, USA and designated ACM-ICH (Hitchcock, 1858, 1865; Rainforth, 2005; Getty et al., 2017). Digital photographs of specimens were converted to greyscale, then regions of surrounding rock in the image were reduced to 50% opacity to enhance the visibility of the track morphology. **Entry** and **exit** features, along with depth zone assignment were determined in Turner et al., 2020.

## **Results**

Guineafowl chose to slow down, speed up, and pause frequently when walking on each of the experimental substrates. This non-steady locomotion provided a broad sampling of kinematic variation from the three individuals. Eighty-one trials were analyzed (64 on deformable substrates), yielding 161 stance phases (114 full, 47 partial).

### **Alternating walking on solid substrates**

On solid surfaces, birds walked using an alternating gait. As shown by a representative trial (Fig. 2), after initial contact (**on**), the focal stance limb (red) remained stable on the surface of the ground until the foot lifted and uDIII broke contact (**off**). Transitions between stance and swing phases were readily identifiable by this abrupt change in uDIII trajectory. The majority of toe motion occurred during swing, when the uDIII paths arced upward and forward before descending to the next stance phase (Fig. 2A). Stance phases on solid surfaces were characterized by two periods of double contact divided by a period of single contact (Fig. 2B). Graphing the vertical position of uDIII through time (Fig. 2C) revealed brief peaks of swing elevation between prolonged troughs of stance phase ground contact. The same pattern is mirrored by the opposite foot (blue), approximately 50% out of phase.

### **Alternating walking on deformable substrates**

When guineafowl walked through the deformable substrates, either dry grains or the spectrum of firm to highly saturated muds, their feet penetrated to a wide range of depths (9-155 mm). Unlike the swing-dominated pattern on the solid substrate, as birds encountered more deformable substrates and sank, a larger fraction of uDIII movement occurred below the ground. Subsurface **entry** and **exit** uDIII paths always differed on the deformable substrates; as described in Turner et al. (2020), these combined motions traced a path in the form of a loop.

With increasing hydration, transitions from swing to stance (**on**) were increasingly blurred as the air-substrate boundary had a decreased impact on foot trajectory or speed. Regardless of substrate, however, transitions from stance to swing (**off**) were seemingly unaffected by the air-substrate boundary, as uDIII paths consistently arced seamlessly from **exit** to swing. These relatively smooth transitions can be seen in one of the deepest and most complete stride cycles captured on the dry granular substrate (Fig. 3A).

uDIII subsurface movements were coordinated with contralateral foot movements, as illustrated by the representative stride cycle in Figure (3). The phase diagram reveals the same pattern as that on solid: prolonged periods of ground contact during stance phase punctuated by brief periods of swing (Fig. 3B). Unlike on solid substrates, where the foot was held at a constant vertical position throughout stance phase (constrained by the solid surface), on deformable substrates the foot sank throughout the majority of the duration of stance (Fig. 3C). This period of **entry** was marked by stepped depth changes over time that typically were coordinated with the opposite foot's movements. Two relatively slow or plateau-like periods of sinking roughly corresponded to double contact, and were separated by a period of rapid descent which corresponded to **exit** and swing of the contralateral foot (Fig. 3D). The relative magnitude of these stepped vertical changes varied, however the majority of **entry** depth was consistently gained prior to the second period of double contact.

### **Conserved proportions of stance depth and loop width**

The prominent loop feature of the uDIII path arises from differential horizontal subsurface foot motion during stance. Forward translation during entry, backward slipping at depth, and posteriorly arcing exit all contribute to total loop width. Despite high variation among the uDIII paths, a relationship in overall loop proportion was identified.

Across all seven deformable substrates, a correlation was found between stance depth (0.90 - 15.49 cm) and loop width (0.06 - 7.37 cm) (Fig. 4). A Pearson product-moment correlation coefficient was computed to assess this relationship for normal alternating walking. A positive correlation was found between the two variables,  $r(79) = .874$ ,  $p < .001$ , with  $R^2$  of 0.764. Loop width was approximately one third of stance depth across substrates. Several observations excluded from the correlation calculation (triangles and squares) represent atypical walking behaviors and are discussed in the last results section.

### **Subdivisions of bipedal gait on deformable substrates and relationship to uDIII loop formation**

As guineafowl walked with alternating steps, a consistent coordinated sequence of kinematic events was found across all substrates (Fig. 5A). When footfall patterns are viewed as a simple phase diagram (Fig. 5B, red and blue bars), the pattern of transitions between double (grey) and single (white) contact on deformable substrates is consistent with that for walking on

solid surfaces. However, feet pass down into deformable substrates to some maximum depth before extraction. Just as the binary presence/absence of foot-ground contact are mechanically relevant locomotor transitions to differentiate, so are within-ground foot sinking and withdrawal. By adding **entry** and **exit** to the phase diagram (black and white bars) of both feet, each period of double contact can be further subdivided (Fig. 5C).

The resulting sequence of kinematic events from both focal (**on**, **maxD**, and **off**) and contralateral (**oppOn**, **oppMaxD**, and **oppOff**) feet are then combined to subdivide a single stance phase into five sub-phases (Fig. 5D). This sequence is found in all alternating walking stance phases. These five kinematic sub-phases mark important exchanges in body support when walking on and through deformable substrates. Each of these unique phases of loading is visible in the directionality of foot movement, and when combined, give rise to the loop form found in uDIII pathlines (Fig. 5E). With reference to Figure 5, we describe foot movements and infer subsurface loading during each phase. The focal (red) stance foot sequentially passes through Sub-Phases 1-5 while the opposite (blue) foot simultaneously traverses Sub-Phases 1'-5'.

**Stance Sub-Phase 1: on - oppMaxD.** After the focal (leading) foot makes initial contact with the substrate, both feet descend until the opposite (trailing) foot reaches maximum depth. As both feet are in contact with the ground and sink throughout this phase, we infer that both are exerting downward force as the focal foot is increasingly loaded. Double foot contact and descent justifies considering this phase “double support”.

**Stance Sub-Phase 2: oppMaxD - oppOff.** The focal foot continues to descend as the opposite foot is withdrawn. From the direction of movement, we infer the focal foot is exerting downward force as the opposite foot is exerting upward force. During this phase, the focal foot is supporting the mass of the animal as well as the forces produced by the opposite foot.

**Stance Sub-Phase 3: oppOff - oppOn.** The focal foot continues to sink as the opposite foot is in swing. Sole focal foot ground contact and descent justifies considering this phase “single support”.

**Stance Sub-Phase 4: oppOn - maxD.** Once the opposite foot makes initial contact with the substrate, both feet descend until the focal foot reaches maximum depth. As both feet are again in contact with the ground and sink throughout this phase, we infer both feet are exerting downward force until the focal foot is fully unloaded. Double foot contact and descent of both feet justifies considering this phase “double support”.

**Stance Sub-Phase 5: maxD - off.** The focal foot is withdrawn as the opposite foot continues to descend. From the direction of movement, we infer the focal foot is exerting upward force as the opposite foot is exerting downward force. During this phase, the opposite foot is supporting the mass of the animal as well as the forces produced by the focal foot.

Thus, uDIII loop trajectory of the focal stance foot on a deformable substrate is formed by a sequence of subterranean motion created through five distinguishable sub-phases of coupled foot interactions spanning three stance phases. The majority of stance phase duration occurs as the focal foot descends during **entry** (Sub-Phases 1-4), which ranged widely in duration (0.50 - 3.29 seconds). This weight-bearing motion during **entry** records two periods of double support: once with the opposite foot trailing, and then again when it is leading. In between, one period of single support occurs as the opposite foot is in swing.

The relatively narrow, widely diverging toes of guineafowl, like most birds, are easily engulfed by substrate after sinking. Thus, the relatively swift (0.02 - 0.84 seconds) withdrawal during **exit** (Sub-Phase 5) entails vertical foot movement back through the same depth of material. This likely provides resistance which the bird partially mitigates by collapsing the foot and reducing surface area during withdrawal. During **exit** the foot rises to the surface from **maxD** at a comparable velocity to swing.

### **Loop complexity from atypical walking behaviors**

In addition to the typical alternating walking, two of the three birds exhibited atypical walking behaviors: kicking and a non-alternating gait (Fig 6). Both of these movements were most obvious in the non-weight-bearing foot: kicks occurring only during **exit**, and non-alternating steps predominantly appearing during **exit** or **swing**. These behaviors break from the described sequence of kinematic events for typical alternating walking, and correspond to additional increases in loop width or step depth.

Kicks were observed when birds walked through semi-liquid muds, in which they sank deeply, and experienced sediment adhering to the foot. In stance phases from six trials, the birds kicked backwards in an apparent attempt to shed material and ease withdrawal. Kicks alter uDIII **exit** direction from a relatively vertical withdrawal to a posterior push and have been observed to occur one to three times during a single exit. Figure (6A-D) shows a sequence of alternating walking where the individual kicked during **exit** in two sequential steps. With each kick, loop width increased.

A non-alternating gait was observed in several steps within five trials across highly deformable substrates, from two of the three birds. In the observed behaviors, instead of the R-L-R-L alternating foot contact pattern, the guineafowl would take a second step with the same foot, resulting in a R-L-L-R or L-R-R-L sequence. Figure (6E-H) shows a sequence of non-alternating walking where an additional mid-swing and mid-exit step was recorded, each penetrating approximately 8 cm. In the case of the mid-swing step, the foot (blue) rapidly paddled through the semi-liquid mud, and did not pause at its own maximum depth before being withdrawn. Thus, the focal stance phase (red) underwent an additional period of double and single contact. At the withdrawal of the opposite (blue) foot from this mid-swing stance phase, the focal (red) foot is seen to sink an additional 2 cm. In the case of the mid-exit step, the foot remained submerged within the sediment as it engaged in a second set of entry and exit motions prior to swing phase.

## **Discussion**

Guineafowl, like many avian and non-avian theropod dinosaurs, are striding bipeds that use alternate hindlimbs to support the body during terrestrial locomotion. To investigate the kinematic origins of subterranean looping foot motions previously documented in these taxa (Turner et al., 2020; Falkingham et al., 2020), we employed biplanar X-ray videography to visualize and measure the sub-surface pedal kinematics. Walking movements sampled across a spectrum of substrate consistencies revealed a conserved sequence of kinematic events. On substrates that yielded to the feet, these phases of gait were drawn out in space and consistently formed a loop. Given insights from these data, we discuss the definition of “stance

phase” on deformable substrates, and the preservation of gait-based information in fossil dinosaur tracks.

### **What is “stance phase” on deformable substrates?**

The kinematic spectrum from swing-dominated foot movements on solid substrates to stance-dominated subsurface foot movements on hydrated muds calls into question the meaning of “stance phase” on deformable substrates. Throughout the period of foot-ground contact in walking bipeds, the foot transmits a variety of decelerative, propulsive, and supportive forces. On relatively stable and unmoving surfaces, these ground-contact interactions are viewed as ‘weight bearing’: contributing vertical forces to support the body against gravity. As such, the walking gait subdivisions of double and single contact are often synonymized with double and single ‘support’.

On deformable substrates, the ground yields to the pedal loads emplaced on it, rendering stance phase as ‘unstable’. In the absence of direct force measurements, the paths taken by the feet are informative about their relative loading. Thus, we can infer that sinking **entry** motions of a foot will meet some vertical resistance (upwards reaction force) from the substrate that may partially support the animal (if it is still sinking, then it is not wholly supported). Conversely, withdrawal (**exit**) motions may be resisted (downwards reaction force), either by collapsed sediment above, and/or cohesive sediment beneath and to the sides of the foot. This fundamental division between **entry** and **exit** during stance phase suggests that ‘contact’ and ‘support’ cannot be equivocated on deformable substrates and that subdivisions of stance phase while the foot remains within the media become increasingly important to consider as more subsurface foot motion is permitted.

In the most deformable substrates, in which the mud was semi-liquid, the birds sank so deeply that their bodies contacted the substrate. When this happens, terms such as ‘support’ or ‘stance’ seem inappropriate, as the substrate is no longer supporting the animal via the foot and leg in the traditional sense. Instead, the animal remains above the sediment surface either through a reduction in pressure resulting from the increased surface area in contact with the substrate, or through buoyancy (or some combination of the two). We were unable to measure forces with our experimental setup, and this phenomenon therefore remains unclear at this time.

Avian step cycles occur on and within a spectrum of media in the natural world. Here we focused on walking, where stance phase is defined by an air-substrate boundary. This is different from wading, where swing occurs within water and stance phase is defined at a water-substrate boundary (Palecek et al., 2021), or from swimming and air stepping where there is no ground contact, and thus no stance phase to divide the cycle (Johnston and Bekoff, 1992). While walking, wading, and swimming are generally seen as distinct locomotor modes, our data show that walking kinematics change considerably as substrate consistency changes and the foot (and bird) sink deeper (Fig. 5), potentially blurring such clear divisions between locomotor modes.

The particularly large looping motions created by the feet in highly deformable, non-supportive substrates are reminiscent of paddling feet during avian swimming (e.g. Johansson and Lindhe Norberg, 2001; Provini et al., 2012; Clifton and Biewener, 2018). Indeed, our mud-based substrates span a continuum from solid, or very firm, to very soft, even semi-liquid in consistency, depending on the water content. In the deepest and most hydrated trials, there

were steps where the foot never fully withdrew from the sediment (e.g. Fig. 6E) and the case could be made that our **entry** and **exit** terms may be homologous to power-stroke and recovery phases of swimming. In terms of the division between walking and swimming, further work is needed to ascertain if there is a continual or abrupt change in kinematics as yet more water is added to turn our semi-liquid substrate into a true fluid with mechanical properties close to those of water.

### **Each track is a record of three footfalls**

As the foot sinks and withdraws from a substrate, a record of three-dimensional foot motion in the form of a footprint or track is left behind (Padian and Olsen, 1984; Gatesy et al., 1999; Manning, 2004; Falkingham et al., 2020). In addition to understanding how the many sources of variation (substrate properties and flow patterns, foot shape and pose, foot motion, and depth sampling within the substrate volume) impact overall track morphology, understanding how the bipedal stride cycle relates to sub-surface looping is critical for building a track-based framework for the study of walking in extinct taxa.

Previously, three phases of walking have been used to describe foot motion during track formation in avian and non-avian dinosaurs: touch-down (T), weight-bearing (W), and kick-off (K) (Thulborn and Wade, 1989), which here approximately equate to **on**, **entry**, and **exit**. While variation in these phases of gait have been recognized as sources of track shape variation (Thulborn and Wade, 1989; Milàn, 2006; Avanzini et al., 2012), most studies on footprint formation have primarily focused on the motions of the focal indenter foot and missed other key events or sub-phases generated by the interaction of both feet.

Data from our guineafowl data visualizations reveal that a track is not made by a single foot in isolation, but rather by the interaction between two feet spanning three stance phases. Specifically, when not in the air, the feet are mechanically coupled through the body as well as through the substrate. For example, the path taken by a focal foot during Sub-Phases 1 and 2 is impacted by the path taken by the trailing, opposite foot during its final stage of descent (Sub-Phase 1') and then ascent (Sub-Phase 2') from the previous footfall. The same kind of interaction takes place during Sub-Phases 4 and 5, which will be affected by the now leading, opposite foot as it descends in the subsequent footfall. The focal foot's path, and thus its footprint, combine aspects of the opposite foot's preceding and following paths.

By viewing track formation as a composite of these sequences of motions, it may be possible to recover information about the bipedal step cycle from fossilized tracks. Deep penetrative tracks (Gatesy and Falkingham, 2017; Novotny et al., 2019; Falkingham et al., 2020; Gatesy and Falkingham, 2020; Turner et al., 2020) made in hydrated substrates are the best candidates for detecting gait-based information, as the subphases are so physically drawn out in space that they have greater potential to be sampled in horizontal fossil slabs. While data here reveals shallow tracks made on relatively firm muds are produced by the same two-footed interactions, the ability to sample and detect fossilized loop features on these substrates is unlikely, because subphases are spatially compressed together.

The preservation of toe motion in penetrative fossil tracks is likely distorted by substrate flow during track formation, as well as by other post formational processes such as post-depositional compression (Gatesy and Falkingham, 2017; Falkingham and Gatesy, 2020).

Despite these challenges, presence of features within a single horizon can be used to build off the tridactyl dinosaur depth zone framework established by Turner et al., (2020) (Fig. 7):

1) The **entry** path in a Zone 1 track likely was created during stance Sub-Phase 1, as this zone occurs between the surface of the ground and the uDIII loop intersection point (e.g., Zone 1 track in Fig. 7).

2) The **entry** path in a Zone 2 track likely was created during stance Sub-Phases 1-3 (e.g., Zone 2 track in Fig. 7).

3) The **entry** path in a Zone 3 track may be created during any of **entry** Sub-Phases 1-4, however in a Zone 3c track, the **entry** path was likely created by Sub-Phase 4, as it is the deepest point of **entry**. Penetrative tracks with scraping claw marks may be a record of this sub-phase (e.g., Zone 3c track in Fig. 7). Future study of the kinematic relationship between all digits on both feet may aid in the ability to better resolve the **entry** sub-phase identification.

4) The **exit** path throughout the entire depth of the track volume was created during Sub-Phase 5.

Thus, a single horizontal fossil track slab contains a record of two discontinuous samples of the stance phase (one **entry** and one **exit**). These **entry** and **exit** features are recognizable and measurable, (Falkingham et al., 2020; Turner et al., 2020) and may aid in the recovery of extinct bipedal gait. Given that the majority of the focal foot stance phase occurred during double foot contact, **entry** and **exit** features of a given fossil track slab are likely formed during two different opposite foot stance phases: the **entry** feature likely created while the opposite foot is in the preceding stance phase, and the **exit** feature created while the opposite foot is in the succeeding stance phase.

Understanding how loop size, depth, and shape are created via the interplay between two legs of a striding biped may be a new path to extracting more nuanced detail of extinct locomotion. Continuing to build upon the looping subsurface foot motion framework with other living avian taxa will shed light on how these relationships shift under different anatomical variables such as body mass, foot shape, and locomotor behavior. This will help us differentiate between core patterns of subsurface foot motion that might pervade walking in all living and extinct dinosaurs, and what might aid in the identification of different locomotor behaviors or taxa. Additionally, this framework may not be limited to bipedal dinosaurs but instead may also extend to primates and other facultative bipeds. As studies in human biomechanics have shown track morphologies reflect patterns of limb kinematics (Raichlen et al., 2010; Hatala et al., 2016; Raichlen and Gordon, 2017), further work identifying shared subsurface foot motion patterns in birds and humans may form a broader foundation for track-based interpretations of bipedal locomotion across dinosaurian and hominin evolution.

## Conclusions

Subsurface foot motions of guineafowl reveal the division of walking gait into stance and swing is insufficient to describe bipedal locomotion on deformable substrates. With increasing substrate deformability, pedal kinematics shift along a continuum from swing-dominated foot movements on solid substrates to stance-dominated subsurface foot movements on semi-liquid muds. By dividing stance phase into 5 sub-phases based on ground contact and maximum

depth events of both feet, the formation of the spatially drawn-out subsurface looping motion can be described and the geometry compared across a wide range of substrates. This two-footed perspective reveals that a single track records the motions of two feet across three stance phases, rather than an isolated interaction between one foot and the ground. This builds upon the loop-based framework of tridactyl track variation, and potentially unlocks more gait-based information preserved in fossil dinosaur tracks than has previously been recognized.

## **Acknowledgements**

We thank our anonymous reviewers and K Padian for constructive feedback on earlier versions of the manuscript. We also thank RE Kambic and TJ Roberts and for help with data collection, D Goldman for creative advice on artificial substrates, and TJ Roberts, AR Manafzadeh, and D Goldman for useful discussion. We gratefully acknowledge the directors and staff of the Beneski Museum of Natural History (L. Allen, T. Harms, D. Jones, A. Martini, H. Singleton, A. Venne, K. Wellspring and S. Williams) for their support.

## **Funding**

This work was supported by the US National Science Foundation (EAR 1452119 to SMG and PLF; IOS 0925077 to SMG; Grant #2030859 to the Computing Research Association for the CIFellows Project to MLT), and the Bushnell Research and Education Fund to MLT.

## **Data Availability**

All calibration images, raw X-ray videos and CT files are available on the XMA Portal:  
[https://xmaportal.org/webportal/larequest.php?request=studyOverview\\_public&StudyID=20&instit=BROWN#collections](https://xmaportal.org/webportal/larequest.php?request=studyOverview_public&StudyID=20&instit=BROWN#collections)

## References

- Allen JRL. 1989. Fossil vertebrate tracks and indenter mechanics. *Journal of the Geological Society*. 146(4):600–602
- Avanzini M, Pinuela L, García-Ramos JC. 2012. Late Jurassic footprints reveal walking kinematics of theropod dinosaurs. *Lethaia*. 45(2):238-52.
- Brainerd EL, Baier DB, Gatesy SM, Hedrick TL, Metzger KA, Gilbert SL, Crisco JJ. 2010. X-ray reconstruction of moving morphology (XROMM): precision, accuracy and applications in comparative biomechanics research. *Journal of Experimental Zoology Part A: Ecological Genetics and Physiology*. 313(5):262-79.
- Clifton GT, Biewener AA. 2018. Foot-propelled swimming kinematics and turning strategies in common loons. *Journal of Experimental Biology*. 221(19):jeb168831.
- Daley MA, Birn-Jeffery A. 2018. Scaling of avian bipedal locomotion reveals independent effects of body mass and leg posture on gait. *Journal of Experimental Biology*. 221(10):jeb152538.
- Ellis RG, Gatesy SM. 2013. A biplanar X-ray method for three-dimensional analysis of track formation. *Palaeontologia Electronica*. 16(1):1T.
- Falkingham PL, Bates KT, Margetts L, Manning PL. 2011. The ‘Goldilocks’ effect: preservation bias in vertebrate track assemblages. *Journal of the Royal Society Interface*. 8(61):1142-54.
- Falkingham PL. 2014. Interpreting ecology and behaviour from the vertebrate fossil track record. *Journal of Zoology*. 292(4):222-8.
- Falkingham PL, Gatesy SM. 2014. The birth of a dinosaur footprint: subsurface 3D motion reconstruction and discrete element simulation reveal track ontogeny. *Proceedings of the National Academy of Sciences*. 111(51):18279-84.
- Falkingham, P.L. and Gatesy, S.M. 2020. Discussion: Defining the morphological quality of fossil footprints. Problems and principles of preservation in tetrapod ichnology with examples from the Palaeozoic to the present by Lorenzo Marchetti et al. *Earth-Science Reviews*, 208, p. 103320. doi:10.1016/j.earscirev.2020.103320.
- Falkingham PL, Turner ML, Gatesy SM. 2020. Constructing and testing hypotheses of dinosaur foot motions from fossil tracks using digitization and simulation. *Palaeontology*. 63(6), 865-880.
- Gage JR, Deluca PA, Renshaw TS. 1995. Gait Analysis: Principles and Applications. *Journal of Bone and Joint Surgery*. 77(10):1607–23.
- Gatesy SM, Middleton KM, Jenkins Jr FA, Shubin NH. 1999. Three-dimensional preservation of foot movements in Triassic theropod dinosaurs. *Nature*. 399(6732):141-4.
- Gatesy SM, Baier DB, Jenkins FA, Dial KP. 2010. Scientific rotoscoping: a morphology-based method of 3-D motion analysis and visualization. *Journal of Experimental Zoology Part A: Ecological Genetics and Physiology*. 313(5):244-61.
- Gatesy SM, Falkingham PL. 2017. Neither bones nor feet: track morphological variation and ‘preservation quality’. *Journal of Vertebrate Paleontology*. May 4;37(3):e1314298.
- Gatesy SM, Falkingham PL. 2020. Hitchcock’s Leptodactyli, penetrative tracks, and dinosaur footprint diversity. *Journal of Vertebrate Paleontology*. 40(3):e1781142.

Getty PR, Olsen PE, LeTourneau PM, Gatesy SM, Hyatt JA, Farlow JO, Galton PM, Falkingham PL, Winitch M. 2017. Exploring a real Jurassic park from the dawn of the age of dinosaurs in the Connecticut Valley. Geological Society of Connecticut, Guidebook 9:1–82.

Hatala KG, Demes B, Richmond BG. 2016. Laetoli footprints reveal bipedal gait biomechanics different from those of modern humans and chimpanzees. *Proceedings of the Royal Society B: Biological Sciences*. 283(1836):20160235.

Hatala KG, Perry DA, Gatesy SM. 2018. A biplanar X-ray approach for studying the 3D dynamics of human track formation. *Journal of Human Evolution*. 121:104–18.

Hitchcock E. 1858 Ichnology of New England: a report on the sandstone of the Connecticut Valley, especially its fossil footmarks, made to the Government of the Commonwealth of Massachusetts. Boston, MA: William White.

Hitchcock, E. 1865. Supplement to the Ichnology of New England: A Report to the Government of Massachusetts, in 1863 (Vol. 385). Wright & Potter.

Hutchinson JR. 2006. The evolution of locomotion in archosaurs. *Comptes Rendus Palevol*. 5(3-4):519-30.

Johansson LC, Lindhe Norberg UM. 2001. Lift-based paddling in diving grebe. *Journal of Experimental Biology*. 204(10):1687-96.

Johnston RM, Bekoff A. 1992. Constrained and flexible features of rhythmical hindlimb movements in chicks: kinematic profiles of walking, swimming and airstepping. *Journal of Experimental Biology*. 171(1):43-66.

Knorlein BJ, Baier DB, Gatesy SM, Laurence-Chasen JD, Brainerd EL. 2016. Validation of XMA Lab software for Marker-based XROMM. *Journal of Experimental Biology*. 219(23):3701–11.

Kuo AD, Donelan JM, Ruina A. 2005. Energetic Consequences of Walking Like an Inverted Pendulum : Step-to-Step Transitions. *Exercise and Sport Sciences Reviews*. 33(2):88–97.

Li C, Zhang T, Goldman DI. 2013. A terradynamics of legged locomotion on granular media. *Science*. 339(6126):1408–12.

Manning PL. 2004. A new approach to the analysis and interpretation of tracks: examples from the dinosauria. *Geological Society, London, Special Publications*. 228(1):93-123.

Milàn J. 2006. Variations in the morphology of emu (*Dromaius novaehollandiae*) tracks reflecting differences in walking pattern and substrate consistency: ichnotaxonomic implications. *Palaeontology*. 9(2):405-20.

Murray MP. 1967. Gait as a total pattern of movement. *American Journal of Physical Medicine & Rehabilitation*. 46(1):290–333.

Novotny J, Tveite J, Turner ML, Gatesy S, Drury F, Falkingham P, Laidlaw DH. 2019. Developing virtual reality visualizations for unsteady flow analysis of dinosaur track formation using scientific sketching. *IEEE transactions on visualization and computer graphics*. 25(5):2145-54.

Padian K, Olsen PE. 1984. The fossil trackway Pteraichnus: not pterosaurian, but crocodylian. *J Paleontology*. 58(1):178–84.

Padian K, Olsen PE, 1989. Ratite footprints and the stance and gait of Mesozoic theropods. Pp. 231–241 in D. D. Gillette and M. G. Lockley, eds. *Dinosaur tracks and traces*. Cambridge University Press, Cambridge

Palecek AM, Novak MV, Blob RW. 2021. Wading through water: effects of water depth and speed on the drag and kinematics of walking Chilean flamingos, *Phoenicopterus chilensis*. *Journal of Experimental Biology*. 224(19):jeb242988.

Provini P, Goupil P, Hugel V, Abourachid A. Walking, Paddling, Waddling: 3 D Kinematics Anatidae Locomotion (*C. allonetta leucophrys*). 2012. *Journal of Experimental Zoology Part A: Ecological Genetics and Physiology*. 317(5):275-82.

R Core Team. 2020. R: A language and environment for statistical computing. R Foundation for Statistical Computing, Vienna, Austria. URL <https://www.R-project.org/>.

Raichlen DA, Gordon AD, Harcourt-Smith WE, Foster AD, Haas Jr WR. 2010. Laetoli footprints preserve earliest direct evidence of human-like bipedal biomechanics. *PLoS one*. 5(3):e9769.

Raichlen DA, Gordon AD. 2017. Interpretation of footprints from Site S confirms human-like bipedal biomechanics in Laetoli hominins. *Journal of Human Evolution*. 107:134-8.

Rainforth E. 2005 Ichnotaxonomy of the fossil footprints of the Connecticut Valley (Early Jurassic, Newark Supergroup, Connecticut and Massachusetts). PhD dissertation, Columbia University, Department of Earth and Environmental Sciences, Manhattan, New York, NY, USA.

Thulborn R, Wade M. 1989. A footprint as a history of movement. In: Gillette, D. D. and Lockley MG, editor. *Dinosaur Tracks and Traces*. Cambridge University Press, New York. p. 51–56.

Turner ML, Falkingham PL, Gatesy SM. 2020. It's in the loop: shared sub-surface foot kinematics in birds and other dinosaurs shed light on a new dimension of fossil track diversity. *Biology Letters*. 16(7):20200309.

Turner ML, Gatesy SM. 2021. Alligators employ intermetatarsal reconfiguration to modulate plantigrade ground contact. *Journal of Experimental Biology*. 224(11):jeb242240.

Verstappen M, Aerts P, Van Damme R. 2000. Terrestrial locomotion in the black-billed magpie: Kinematic analysis of walking, running and out-of-phase hopping. *Journal of Experimental Biology*. 203(14):2159–70.

Whittle MW. 1996. Clinical gait analysis: A review. *Human Movement Science*. 15(3):369–87.

Winter DA. 1980. Overall principle of lower limb support during stance phase of gait. *Journal of Biomechanics*. 13(11):923–7.

## Figure Legends

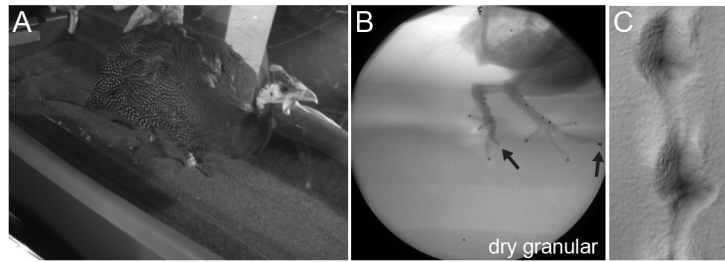


**Figure 1. Standard and X-ray video frames of guineafowl feet during stance phase on the dry granular substrate. (A)** In oblique view, the foot sinks below the surface of this substrate and is not visible. **(B)** In the X-ray video, foot and markers under the unguis of digit III (indicated by black arrows) are visible underground. **(C)** Photogrammetry model of a trackway made in the dry grains. Scale bar equals 5 cm for tracks.

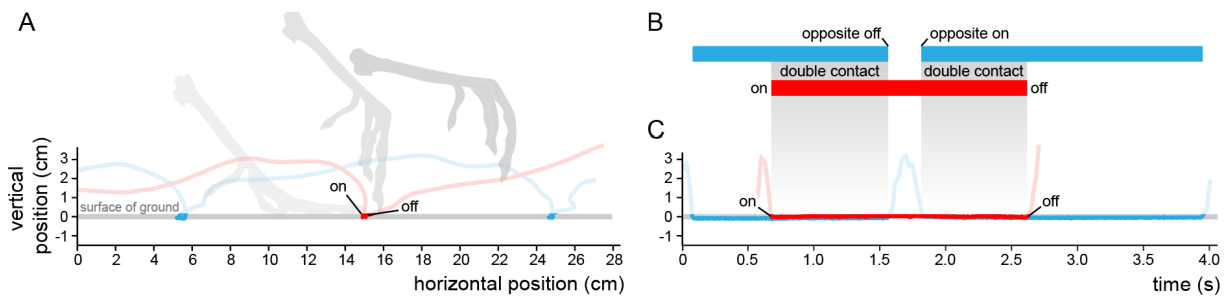


**Figure 2. Guineafowl uDIII motion during alternating walking on a solid substrate. (A)** Vertical and horizontal position of uDIII on the focal stance foot (red) and opposite foot (blue) in right lateral view. **(B-C)** Temporal breakdown of data presented in **(A)**. **(B)** Phase diagram showing stance phases through time. Red and blue bars represent individual foot contacts. Periods of double contact indicated in grey. **(C)** Vertical position over time. Peaks indicate periods of swing (semi-transparent) punctuating flat traces of the ground contact during stance (opaque).

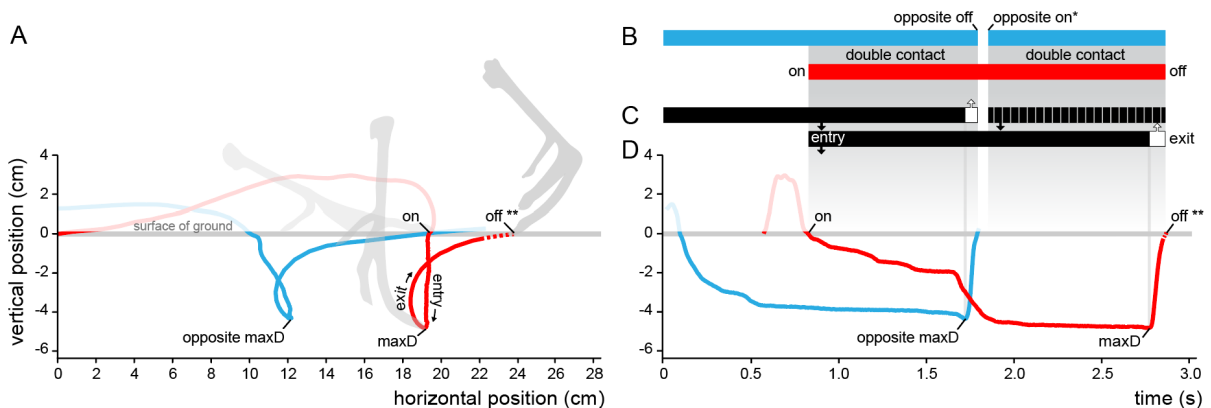


**Figure 3. Guineafowl uDIII motion during alternating walking on a dry granular substrate. (A)** Vertical and horizontal position of uDIII on the focal stance foot (red) and opposite foot (blue) in right lateral view. **(B-D)** Temporal breakdown of data presented in **(A)**. **(B)** Phase diagram showing stance phases through time. Red and blue bars represent individual foot contacts. Periods of double contact indicated in grey. **(C)** Black and white bars represent the division of the stance phases into **entry** (black) and **exit** (white) components. **(D)** Vertical position over time. Peaks indicate periods of swing (semi-transparent) punctuating descending and ascending subsurface traces of ground contact during stance (opaque). \* = kinematic event time identified from light video only. \*\* = projected uDIII position, kinematic event not visible in X-ray volume. Dashed bars represent inferred direction of foot motion in the absence of X-ray data.

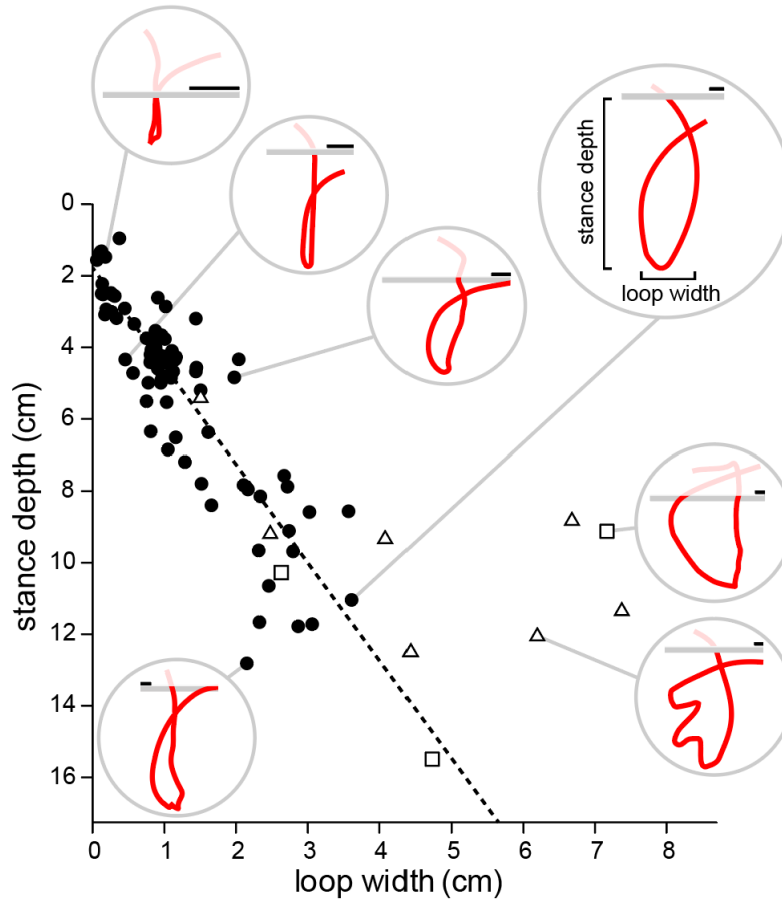
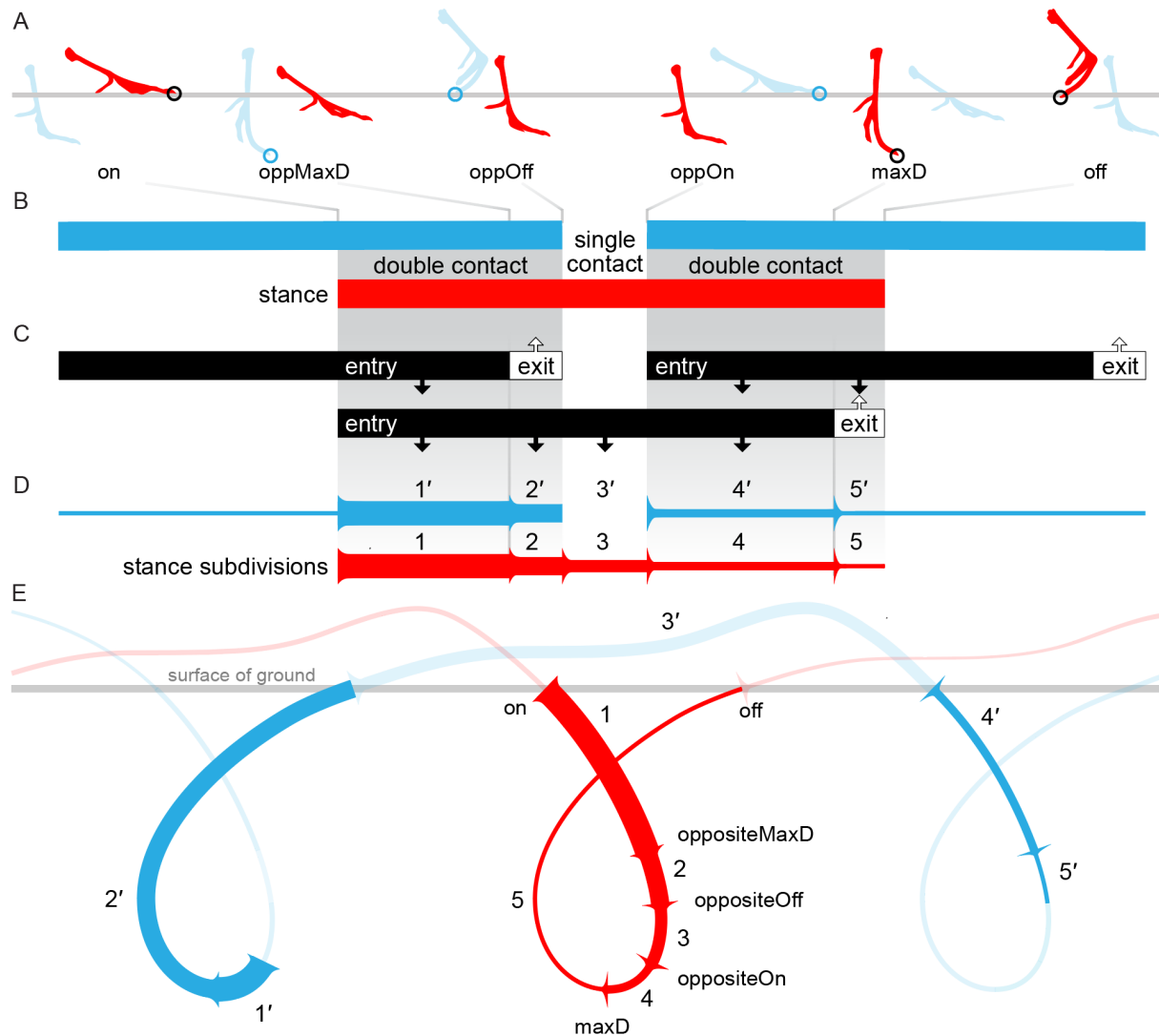


**Figure 4. Relationship of loop width and step depth measured from guineafowl uDIII paths during stance phase on all deformable substrates.** Sample uDIII trajectories (red) in right lateral view with leader line associated with data point on graph. Observations of stance phases involved in the atypical walking behaviors of non-alternating walking (squares) and kicks (triangles) are indicated. Loop width and step depth are found to be strongly positively correlated for stance phases of typical alternating walking behaviors (solid circles),  $r(79) = .874$ ,  $p < .001$ , with  $R^2$  of 0.764. Scale bars equal 1 cm.



h

**Figure 5. The five subdivisions of stance phase on deformable substrates. (A)** Snapshots of the focal limb (red) and contralateral limb (blue) at notable kinematic events throughout a single stance phase. **(B)** Phase diagram showing stance phases through time. Red and blue bars represent individual foot contacts. Periods of double contact indicated in grey. **(C)** The division of double contact into two discrete periods: first, both feet actively sinking during **entry** (each represented by a black down arrow), and second, a transitional period when one foot pulls out during **exit** (represented by a white up arrow) while the other foot continues to sink. **(D)** Phase diagram combining (B) and (C) showing the five subdivisions of stance phase. Synchronous phases of the opposite foot are marked with a prime symbol, and decrease in line thickness. **(E)** Loop diagram indicating the spatial relationship of phases in (D) as determined by kinematic events from focal (**on**, **maxD**, **off**) and opposite (**oppMaxD**, **oppOff**, **oppOn**) feet.

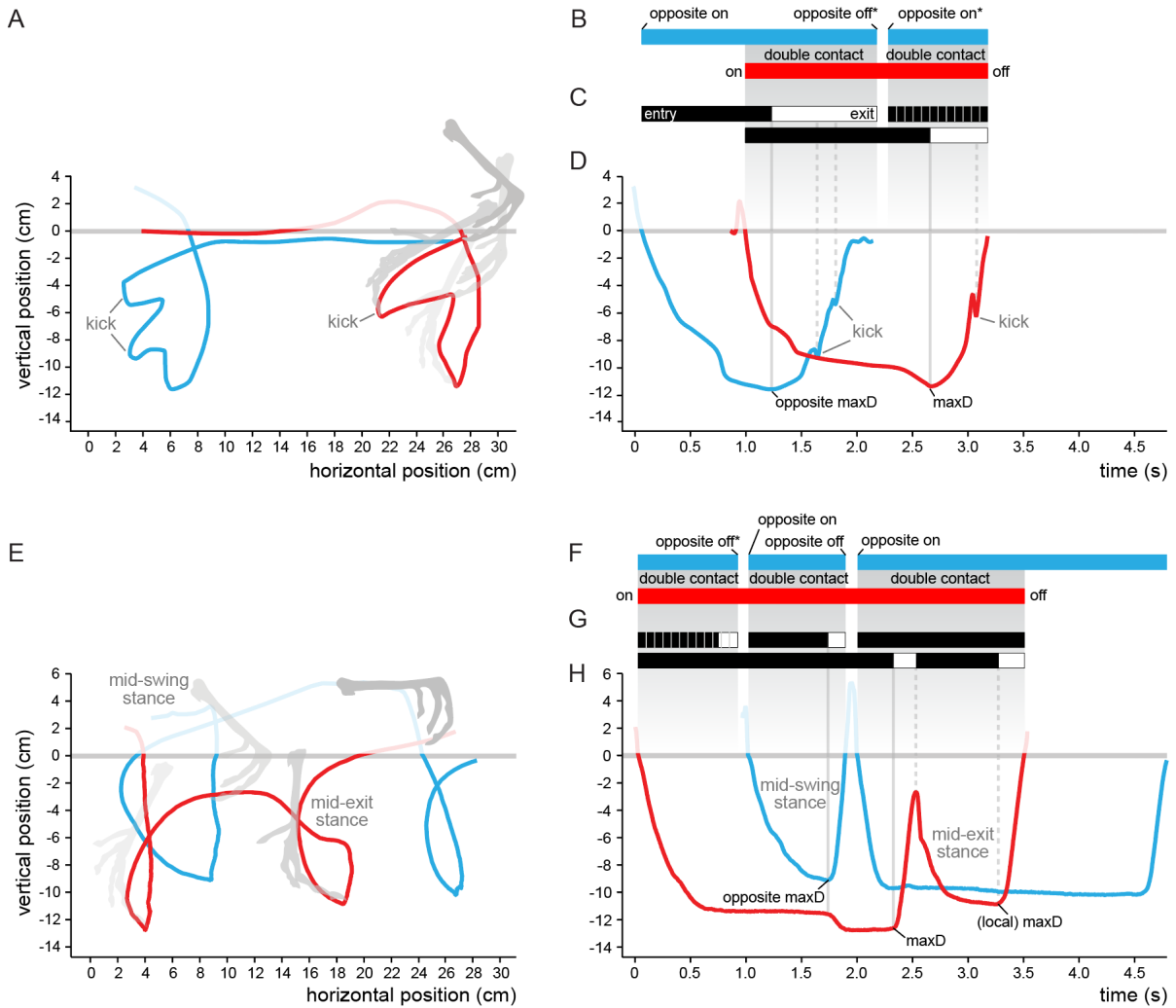


**Figure 6. Examples of atypical walking behaviors.** (A-D) Kicks during *exit* and (E-H) non-alternating mid-swing and mid-exit steps. (A) Vertical and horizontal position of uDIII on the focal stance foot (red) and opposite foot (blue) in right lateral view. (B-D) Temporal breakdown of data presented in (A). (B) Phase diagram showing stance phases through time. Red and blue bars represent individual foot contacts. (C) Black and white bars represent the division of the stance phases into *entry* (black) and *exit* (white) components. (D) Vertical position over time. Peaks indicate periods of swing (semi-transparent) punctuating descending and ascending subsurface traces of ground contact during stance (opaque). (E) Vertical and horizontal position of uDIII on the focal stance foot (red) and opposite foot (blue) in right lateral view. (F-H) Temporal breakdown of data presented in (E). (F) Phase diagram showing stance phases through time. Red and blue bars represent individual foot contacts. (G) Black and white bars represent the division of the stance phases into *entry* (black) and *exit* (white) components. (H) Vertical position over time. Peaks indicate periods of swing (semi-transparent) punctuating descending and ascending subsurface traces of ground contact during stance (opaque). Periods of double contact indicated in grey. \* = kinematic event time identified from light video only. Dashed bars represent inferred direction of foot motion in the absence of X-ray data.

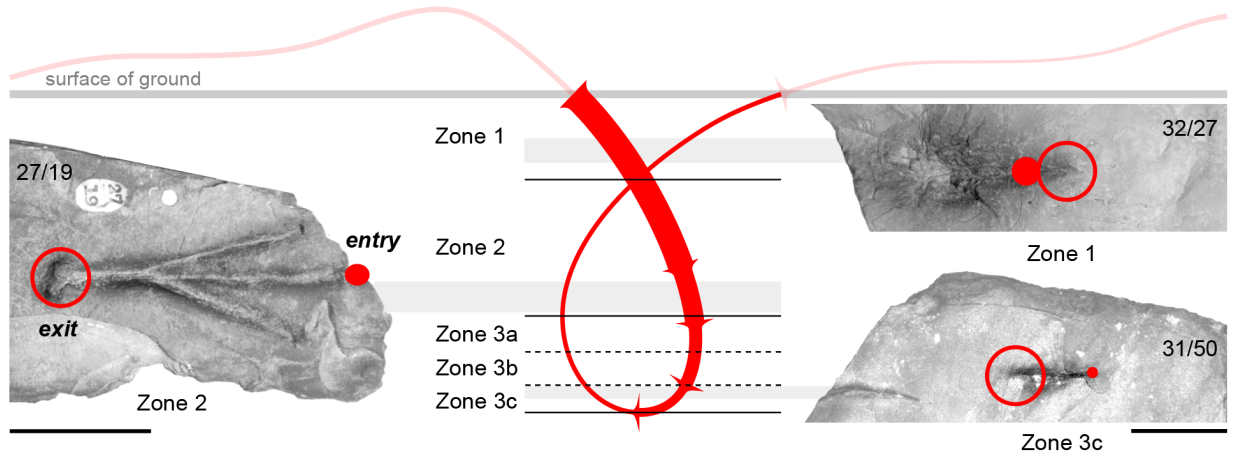


**Figure 7. Stance sub-phase identification from uDIII *entry* and *exit* features in Early Jurassic fossil dinosaur tracks. *Entry* (filled circles) and *exit* (open circles) features and depth zone assignment were determined in Turner et al., 2020. See Figure 5 for details on each stance sub-phase. ACM-ICH specimen numbers displayed in upper corners of each fossil. Scale bars equal 5 cm.**